Parkin May 2018.docx

Parkin is required for exercise-induced mitophagy in muscle: impact of aging

Chris Chin Wah Chen[1,2], Avigail T. Erlich[1,2], Matthew J. Crilly[1,2] and David A. Hood[1,2]

[1]School of Kinesiology and Health Science,
[2]Muscle Health Research Centre，
York University, Toronto,
Ontario M3J 1P3, Canada

To whom correspondence should be addressed: David A. Hood, PhD
School of Kinesiology and Health Science
York University, 4700 Keele St.,
Toronto, Ontario
M3J 1P3, Canada
Tel: (416) 736-2100 ext: 66640
E-mail: dhood@yorku.ca

Running title: Parkin-mediated mitophagy in aged skeletal muscle

Keywords: Mitochondrial biogenesis, mitophagy flux, ubiquitination, reactive oxygen species, PGC-1α, PARIS

ABSTRACT

The maintenance of muscle health with advancing age is dependent on mitochondrial homeostasis. While reductions in mitochondrial biogenesis have been observed with age, less is known regarding organelle degradation. Parkin is an E3 ubiquitin ligase implicated in mitophagy, but few studies have examined Parkin's contribution to mitochondrial turnover in muscle. Wild type (WT) and Parkin knockout (KO) mice were used to delineate a role for Parkin-mediated mitochondrial degradation in aged muscle, in concurrence with exercise. Aged animals exhibited declines in muscle mass and mitochondrial content, paralleled by a nuclear environment endorsing the transcriptional repression of mitochondrial biogenesis. Mitophagic signaling was enhanced following acute endurance exercise in young WT mice, but was abolished in the absence of Parkin. Basal mitophagy flux of the autophagosomal protein LC3II was augmented in aged animals, but did not increase additionally with exercise when compared to young animals. In the absence of Parkin, exercise increased the nuclear localization of PARIS, corresponding to a decrease in nuclear PGC-1α. Remarkably, exercise enhanced mitochondrial ubiquitination in both young WT and KO animals. This suggested compensation of alternative ubiquitin ligases that were, however, unable to restore the diminished exercise-induced mitophagy in KO mice. Under basal conditions, we demonstrated that Parkin was required for mitochondrial Mfn2 ubiquitination. We also observed an abrogation of exercise-induced mitophagy in aged muscle. Our results demonstrate that acute exercise-induced mitophagy is dependent on Parkin, and attenuated with age, which likely contributes to changes in mitochondrial content and quality in aging muscle.

INTRODUCTION

Mitochondria have emerged as an important nexus of stress within the cell. Including their canonical function as energy producers, mitochondria also exhibit pleiotropic roles in regulating metabolic signaling. In a tissue such as muscle, mitochondria can respond to sustained energetic requirements by increasing organelle content via a process termed mitochondrial biogenesis. This expansion is critical for muscle adaptation to occur in response to exercise training (19). A plethora of studies have established the broad beneficial effects of exercise, but the molecular mechanisms that accompany improved muscle quality remain obscure. Recent research has suggested that autophagy is a possible mechanism for potentiating muscle plasticity in response to exercise (18, 62).

Autophagy is a catabolic, evolutionary-conserved process involved in the engulfment of dysfunctional organelles and protein aggregates. Mitophagy is a specific form of autophagy, accountable for the elimination of dysfunctional mitochondria following damage or stress. Once an entire mitochondrion becomes depolarized, organelle fragmentation permits mitophagy to eliminate the dysfunctional segment from the mitochondrial reticular network (7, 61, 65). This change in mitochondrial morphology is initiated and regulated in part by the E3 ubiquitin ligase Parkin (12, 48). Under non-stressful conditions, mitochondrial PTEN-induced putative kinase 1 (PINK1) is rapidly imported into the organelle and degraded by the inner mitochondrial membrane rhomboid protease presenilin-associated rhomboid-like protein (PARL) (25). When a mitochondrion encounters a loss in membrane potential, PINK1 stabilizes and accumulates on the outer mitochondrial membrane to selectively recruit Parkin (32, 42). The mitochondrial translocation of Parkin induces ubiquitin localization on outer mitochondrial membrane targets, and is further activated by PINK1 phosphorylation of ubiquitin (27, 28, 30). Adapter protein sequestosome 1 (p62) interacts with mitochondrial ubiquitin and with microtubule-associated protein light chain 3 (LC3) on the autophagic phagophore membrane (2, 46). These tagged dysfunctional mitochondria are encapsulated into autophagosomes and sequestered to the lysosome for proteolytic degradation.

In muscles with disrupted autophagic signaling, pathology entailing disorganized swollen mitochondria is displayed (38). This suggests that mitophagy may have a role in the preservation of organelle content and function in muscle. While work has been done on Parkin in muscle on lower model organisms (16, 49) and in cell culture (50), the physiological function of Parkin in mammalian skeletal muscle function, and in response to physiologically relevant stressors such as exercise, remains unknown. Recent studies have investigated the influence of autophagy activation in skeletal

muscle following a bout of endurance exercise (17, 18, 51, 62). We have previously demonstrated that mitochondrial Parkin localization is enhanced in response to acute exercise (62). Therefore, in this study, we sought to examine Parkin's role in skeletal muscle function, and whether Parkin is required for acute exercise-induced mitophagy flux using a Parkin KO mouse model.

Similar to the phenotype of autophagy deficiency, aged muscle displays an accumulation of dysfunctional mitochondria in lysosomal lipofuscin bodies (44). Aged animals also demonstrate an elevated amount of mitochondrial ROS emission (6), which can perpetuate organelle damage. Indeed, autophagy inhibition in muscle can elicit a reduction in muscle contractile activity due to non-autophagocytosed mitochondria (38). This notion is part of the mitochondrial-lysosomal axis theory of aging that postulates that increasing organelle dysfunction irreversibly leads to the deterioration of post-mitotic cells (4). In skeletal muscle, this process is manifested as sarcopenia, which is characterized by the age-related loss of muscle function and strength (5, 36), and a reduced transcriptional drive for mitochondrial biogenesis (6). Yet, the selective degradation of mitochondria and its role with advancing age remains unclear. We have previously shown that the expression of autophagy proteins and their localization to mitochondria are not decreased, but rather that the induction of mitophagy remains impaired in aged muscle (44). Interestingly, the overexpression of Parkin has been shown to enhance mitophagic flux and extend lifespan in lower model organisms (49). Thus, we hypothesized that Parkin may play an increasing role in regulating skeletal muscle function and mitochondrial degradation with age. The aims of our study were to investigate: 1) the role of Parkin in acute exercise-induced mitophagy, and (2) possible age-related alterations in mitophagic flux brought about by endurance exercise.

MATERIALS AND METHODS

Mice. C57BL/6 (WT) and B6; 129S4-Park2^{tm1Shn}/J (Parkin KO) mice (Jackson Labs, 006582) were housed in a 12 h light–dark cycle room and allowed access to food and water *ad libitum*. The generation of these mice has been previously described (14). Progeny were genotyped by obtaining ear clippings for DNA extraction. DNA was subsequently incubated with JumpStart REDtaq polymerase (Sigma-Aldrich, St. Louis, MO) along with forward and reverse primers for the WT or altered Parkin gene. These products were amplified using PCR and separated on a 1.5% agarose gel containing ethidium bromide for visualization the genotype. The minimum age threshold for young and aged conditions were 3 and 18 months, respectively.

Exercise Protocol and Blood Lactate. To evaluate mitophagy flux, animals were administered colchicine, or an equal amount of vehicle (water), via intraperitoneal injections every 24 hours (0.4 $mg \cdot kg^{-1} \cdot day^{-1}$) (26) for 2 days prior to the day of exercise and euthanization. After 2 days of habituation on the treadmill, along with the vehicle or colchicine injections, animals in the exercise (Ex) and exercise and 2 hours recovery (ExR) groups were subjected to exhaustive treadmill exercise on a 10° incline. Young WT and KO animals ran at 0 m/min for 5 minutes, 5 m/min for 5 minutes, 10 m/min for 10 minutes, 15 m/min for 15 minutes, 20 m/min for 20 minutes followed by incremental exercise at 1 m/min for every 1 minute until to failure. Aged WT and KO animals ran a similar protocol but Ex groups began incremental exercise after 10 m/min for 10 minutes. There were no ExR groups for aged WT and KO animals due to a lower sample size. The exercise bout ended when animals appeared visibly exhausted and could not continue, even in the presence of air jet stimulation. Metabolic stress was also assessed by measuring blood lactate from a small tail bleed using the Lactate Scout+ analyzer (EKF Diagnostics, Magdeburg, Germany). All animals were sacrificed by cervical dislocation immediately after exercise (Ex), or 2 hours postexercise (ExR). All animal protocols were submitted and approved by the York University Animal Care Committee. Animals were treated in accordance with Canadian Council of Animal Care guidelines.

Muscle Extraction and Cytochrome c Oxidase (COX) Enzyme Activity. The quadriceps muscle was surgically removed and immediately freeze-clamped with metal tongs pre-cooled in liquid nitrogen and subsequently weighed and stored at –80 °C for future use. Frozen muscle samples were pulverized into powder, then dissolved in whole muscle extraction buffer, followed by sonication and centrifugation. Supernatant fractions were recovered and protein content was determined by the

Bradford technique. In addition, COX activity measurements were performed on young and aged groups of Parkin KO and WT mice to measure whole muscle mitochondrial content. Briefly, whole muscle extracts were added to a test solution containing fully reduced cytochrome c. Enzyme activity was determined by the maximal oxidation rate of completely reduced cytochrome c, evaluated as the rate of change in absorbance at 550 nm using a Synergy HT microplate reader, as previously described (39). The data were gathered and calculated using KC4 software.

Mitochondrial Isolation. Mixed hindlimb muscles were immediately placed into ice-cold mitochondrial isolation buffer, followed by mincing and homogenization. Intermyofibrillar (IMF) mitochondrial subfractions were fractionated by performing differential centrifugation, as described previously (9, 39, 52, 67). Mitochondria were resuspended in 100mM KCl, 10mM MOPS, and 0.2% BSA. Freshly isolated mitochondria were used for mitochondrial respiration and reactive oxygen species (ROS) emission assays, and aliquots of mitochondrial extracts were stored at –80ºC for mitochondrial co-immunoprecipitation assay and immunoblotting analyses. The protein concentration values of the isolated mitochondria were determined using the Bradford method.

Mitochondrial Respiration and ROS Production Assay. Basal IMF mitochondrial respiration (state 4) rates were performed in the presence of 10 mM glutamate (Sigma) followed by the addition of 0.44 mM ADP (state 3, Sigma). During state 3, NADH was added to ensure intact inner mitochondrial membrane integrity. No differences in respiration rates were observed when NADH was added to isolated mitochondria samples. All respiration rates were performed using the Mitocell S200 Micro Respirometry System (Strathkelvin Instruments, North Lanarkshire, UK). ROS emission was measured using isolated mitochondria from WT and Parkin KO mice that were incubated in a 96 well plate with VO2 buffer (in mM: 250 sucrose, 50 KCl, 25 Tris, and 10 K2HPO4, pH 7.4) at 37 °C for 30 minutes under state 4 and 3 conditions. 2',7'-dichlorodihydrofluorescein diacetate (50 µM H2DCFDA, ThermoFisher) was subsequently added and fluorescence between 480 and 520 nm was measured on a Bio-Tek Synergy HT microplate reader to directly measure ROS emission. ROS emission was expressed per nanoatom of O2 consumed, as measured during mitochondrial respiration.

Nuclear and Cytosolic Fractionation. Freshly isolated tibialis anterior muscle was removed in Con, Ex, and ExR groups and placed into ice-cold phosphate buffered saline containing protease inhibitor cocktail complete, ETDA-free (Roche Applied Science) and phosphatase inhibitor cocktail

(Sigma). Nuclear and cytosolic components were obtained using a commercially available NE-PER Nuclear and Cytoplasmic Extraction Reagents kit (ThermoFisher), according to the manufacturer's instructions.

Mitochondrial Co-immunoprecipitation Assay. Isolated IMF mitochondrial fractions were solubilized with 1% Triton X-100 and supplemented with protease and phosphatase inhibitor cocktails. Mitochondria were incubated with anti-Mfn2 (M6444, Lot No. 103M4780, Sigma) overnight at 4°C on a nutator mixer, and the supernatant was collected by centrifugation at 12,000 *g* for 10 minutes at 4°C. The following day protein A/G plus-agarose immunoprecipitation reagent (sc-2003, Santa Cruz) was added to the mixture and incubated for 1 hour at 4°C on a nutator mixer. The supernatant fraction was removed from the beads after centrifugation, representing unbound proteins. The collected beads were washed three times and eluted three times with 50 µl of SDS-PAGE gel loading buffer to obtain the maximum elution of purified complexes. Co-immunoprecipitates were used for immunoblot analysis for ubiquitin (SPA-203, Lot No. 1051534, Enzo Life Sciences). Anti-IgG antibody was used as a non-specific control.

Immunoblotting. Muscle extracts and isolated nuclear, cytosol and mitochondrial fractions were separated using SDS-PAGE (12-15% polyacrylamide) and later electroblotted onto nitrocellulose membranes. Membranes were blocked with 5% skim milk in TBST (Tris-buffered saline-Tween 20, 25 mM Tris HCl (pH 7.5), 1 mM NaCl, and 0.1% Tween 20) solution for 1 hour at room temperature. Next, blots were incubated with primary antibodies against LC3/microtubule-associated protein light chain 3 (4108, Lot No. 3, Cell Signaling), p62/sequestosome 1 (P0067, Lot No. 015M4877V, Sigma), ubiquitin (SPA-203, Lot No. 1051534, Enzo Life Sciences), Parkin (4211, Lot No. 4, Cell Signaling), PGC-1α/peroxisome proliferator-activated receptor-γ coactivator-1α (ab3242, Lot No. 2691399, Millipore), PARIS/parkin-interacting substrate (ab130867, Lot No. GR235090-1, abcam), H2B/histone 2B (2943S, Lot No. 4, Cell Signaling), VDAC/voltage-dependent anion channel (ab14734, Lot No. GR121056-7) and α-tubulin (CP06, Lot No. D00175772, Millipore) overnight at 4 °C. On the next day, the blots were rinsed three times in TBST, followed by a 1 hour incubation period at room temperature with appropriate horseradish peroxidase-conjugated secondary antibodies. The blots were again washed three times in TBST and visually detected using enhanced chemiluminescence (Clarity ECL Western blotting substrates, Bio-Rad, CA) and photographic film.

Of note, the top band of p62 was quantified when two bands were visible. Films were then scanned and quantified using ImageJ software (Version 1.48, NIH, USA).

Statistical Analysis. Data were analyzed with Graph Pad 6.0 software, and values are reported as means ± SEM. For mitophagy flux, individual lanes representing LC3II and p62 were first corrected for loading, and then the difference in band intensity between the colchicine- and the vehicle-treated animals was calculated within each immunoblot. Data were analysed using two-way analysis of variance (ANOVA) on the two factors (Genotype and Exercise), except for Fig. 1A which was analysed using a student's t-test. For all two-way ANOVA analyses, Tukey's post hoc test was used to identify individual differences when statistical significance was observed. Statistical differences were considered significant if $P < 0.05$.

RESULTS

Aged mice exhibit reduced whole muscle mass and mitochondrial content. To determine the role of Parkin and age in skeletal muscle, we first assessed the anatomical characteristics of young and aged groups of WT and Parkin KO animals. Total body mass did not differ between WT and KO mice, but both genotypes displayed a 1.6- and 1.8-fold increase in body mass with age, respectively ($P = 0.0001$; Table 1). Quadriceps muscle mass did not differ between young animals, while aged WT and KO animals exhibited 12% decreases in whole quadriceps muscle mass when corrected for tibia length, compared to young mice (Table 1). Thus, we attribute the age-related increase in body mass to an increase in body fat, as illustrated by the significant ~8-fold increase in epididymal fat mass when corrected for total body mass, irrespective of genotype ($P = 0.0001$; Table 1). In addition, we measured Parkin protein expression in young and aged whole quadriceps muscle. We found a robust ~4-fold increased expression of Parkin in aged, compared to young muscle ($P = 0.03$; Fig. 1A). Whole muscle mitochondrial content was assessed by using a cytochrome c oxidase (COX) activity assay. There was no difference between young WT and KO animals, and both genotypes exhibited similar decrements of ~40% with age ($P = 0.004$; Fig. 1B).

We also examined state 4 and glutamate/pyruvate-driven state 3 mitochondrial respiration. No effect of age was observed. When young animals were compared, no differences between genotypes were noted in state 4 respiration, however a 20% decrease in state 3 mitochondrial respiration was detected in KO mice compared to WT counterparts ($P = 0.04$; Fig. 1C). In young WT and KO

animals, no difference in ROS emission was observed under state 4 and 3 conditions. However, with age, Parkin KO animals displayed a ~2.7-fold increase in state 4 ROS production, when compared to WT animals (P = 0.01; Fig. 1D).

Aging results in reduced exercise performance and mitochondrial Parkin localization, along with increased acidosis. We next investigated the role of Parkin with aging and exercise performance. In young WT animals, we found a 1.5-fold increase in Parkin localization to mitochondria immediately following an acute bout of exercise (P = 0.03; Fig. 2A). Parkin localization on mitochondria was severely reduced with age, and the exercise-induced response was abolished (P = 0.0001; Fig. 2A). To determine Parkin's requirement in endurance performance, we subjected young and aged groups of WT and KO mice to a bout of acute, prolonged exercise. No significant differences were detected for total distance run between young WT and KO animals, and both genotypes exhibited elevated blood lactate concentrations of ~8 mM immediately following exercise (P = 0.0001; Fig. 2C). Aged mice ran only 25% of the distances of their younger counterparts (P = 0.0001; Fig. 2B), and this response was accompanied by 1.5-2-fold higher exercise-induced increases in blood lactate levels with age (P = 0.0001; Fig. 2C).

Mitophagy flux is induced following exercise, but this signaling is attenuated in the absence of Parkin. To evaluate a role for Parkin on mitophagy during exercise, mice were subjected to acute exercise to induce mitophagy flux. Following each condition (rest, exercise or exercise and recovery), mitochondria were isolated from the hindlimb muscles of mice to examine the mitochondrial localization of autophagy proteins. With exercise, mitochondrial localization of LC3II increased by 2.8-fold (P = 0.01; Fig. 3A and 3B) in young WT mice, which remained elevated during recovery. This was paralleled by a 2.4-fold increase in mitochondrial p62 localization in young WT mice with exercise (P = 0.02; Fig. 3A and 3C). Mitochondrial LC3II and p62 did not significantly increase with exercise, or during recovery, in young KO animals.

Mitophagy flux of LC3II and p62 was corrected for using VDAC as a loading control and then the calculated as the difference between colchicine- and vehicle-treated animals. Our results indicate that basal mitophagy LC3II and p62 flux was not significantly different between young WT and KO animals. During exercise, mitochondrial LC3II flux was elevated by 3.9-fold in young WT animals (P = 0.01; Fig. 3A and 3D). This was attenuated in the absence of Parkin. We also detected a 2-fold

increase in p62 flux in young mice with exercise (P = 0.02; Fig. 3A and 3E). These data indicate that exercise can induce mitophagic flux, and that the magnitude of this increase is Parkin-dependent.

Mitophagy flux is enhanced with age but does not increase additionally with acute exercise. We then directly compared the role of Parkin-mediated mitophagy between young and aged animals. In aged WT animals, basal LC3II and p62 flux were significantly higher, when compared to young WT animals (P = 0.005; Fig. 4A–C). With exercise, LC3II flux and p62 flux in aged WT animals did not increase additionally when compared to young WT animals (Fig. 4A–C). In the absence of Parkin, basal LC3II (P = 0.0001; Fig. 4D, 4E and 4G) and p62 flux (P = 0.0002; Fig. 4D, 4F and 4H) were both significantly elevated in aged mice, compared to young KO animals (Fig. 4D–H), and were not significantly different following exercise (Fig. 4D–F). Furthermore, the magnitude of basal LC3II flux was significantly higher in aged KO, compared to aged WT animals (P = 0.04; Fig. 4G). Our data indicate that mitophagic signaling is enhanced within aged muscle, and this effect may reduce the potentiation of exercise on mitophagy flux.

Acute exercise induces mitochondrial ubiquitination in young animals, but is attenuated with age. To assess the potential role of Parkin in exercise-induced protein ubiquitination, we examined global ubiquitination on isolated mitochondrial fractions from young WT and KO animals. Basal ubiquitin flux did not differ between genotypes (Fig. 5A and 5B). Ubiquitin flux increased by ~4.1-fold in young WT, immediately following exercise (P = 0.0001; Fig. 5A and 5B), corresponding with the increase in Parkin localization on mitochondria in young WT animals. Remarkably, mitochondrial ubiquitination was also similarly increased by exercise in young KO animals (P = 0.0001; Fig. 5A and 5B). We also found that ubiquitin flux returned to baseline during recovery in young animals (Fig. 5A and 5B). In aged muscle, there were also no differences in basal ubiquitin flux on isolated mitochondria between WT and KO animals (Fig. 5C and 5D). However, in contrast to young animals, ubiquitin flux was considerably higher with age (compare control conditions in Fig. 5D vs 5B), and the effect of acute exercise to increase mitochondrial ubiquitination was completely abolished (Fig. 5C and 5D).

We extended this analysis further to assess the potential function of Parkin on the ubiquitination of specific proteins during exercise. We evaluated Mitofusin-2 (Mfn2) ubiquitination, a known outer mitochondrial membrane target of Parkin, using mitochondrial co-immunoprecipitation to resolve Mfn2-ubiquitin complexes following exercise in young and aged Parkin KO and WT mice. The basal

formation of Mfn2-ubiquitin complexes was significantly reduced by 52% in young KO animals, relative to young WT controls (P = 0.04; Fig. 5E and 5F). Consistent with the translocation of Parkin to the mitochondria with exercise, we found that exercise significantly enhanced Mfn2 ubiquitination on mitochondria of young animals by ~2-fold, relative to young WT control animals (P = 0.01; Fig. 5F). With age, Mfn2 ubiquitination was increased basally by ~2-fold (P = 0.01; Fig. 5E and 5F), in both WT and KO counterparts. This ubiquitination remained unchanged with exercise (Fig. 5E and 5F). These data indicate that Parkin is involved in maintaining basal mitochondrial protein ubiquitination in muscle, and that exercise can promote protein ubiquitination even in the absence of Parkin, in young animals.

PGC-1α and PARIS localization to the nucleus are negatively correlated in response to exercise in young animals, but this relationship is abolished with age. Parkin is not only involved in the ubiquitination of mitochondrial proteins but has also been shown to regulate the levels of transcriptional regulators, such as Parkin interacting substrate, PARIS. It is known that PARIS transcriptionally represses PGC-1α, known as the master regulator of mitochondrial biogenesis, in the absence of Parkin. Interestingly, the basal levels of PARIS localized to the nucleus did not differ between young WT and KO animals (Fig. 6A and 6B). In aged animals, nuclear PARIS localization, when corrected for total PARIS content, was 1.3-2-fold higher in KO and WT animals, when compared to young counterparts (P = 0.0004; Fig. 6A and 6B). Similarly, nuclear PGC-1α abundance was not affected by the absence of Parkin, but was reduced by 35-40% in aged WT and KO mice (P = 0.004; Fig. 6A and 6C).

We next explored if exercise could influence the subcellular localization of these transcriptional regulators. A significant interaction between genotype and exercise on nuclear PARIS localization was found in young animals (P = 0.04; Fig. 7A and 7C). With acute exercise, nuclear PARIS localization diminished in WT animals, but was enhanced in the nuclear fractions of mice lacking Parkin. A similar interaction was found for PGC-1α in the nucleus of young mice following exercise (P = 0.005; Fig. 7A and 7E). PGC-1α increased significantly by 2.2-fold in the nucleus of WT animals, immediately after exercise (P = 0.01; Fig. 7A and 7E). This exercise-induced increase of nuclear PGC-1α abundance was completely negated in the absence of Parkin. In aged animals, nuclear PGC-1α and PARIS remained unchanged following exercise (Fig. 7B, 7D and 7F). These

data suggest that exercise can induce the translocation of PGC-1α and PARIS but that this is qualitatively different in the absence of Parkin, and abolished with age.

DISCUSSION

Sarcopenia is defined as a loss of muscle mass and strength that occurs with age (24). It is established that sarcopenia is governed, in part, by lowered mitochondrial content (6, 36, 44) and reduced transcriptional regulation towards mitochondrial biogenesis (35). Although much is known about the synthesis of mitochondria, fewer studies have examined mitochondrial degradation (i.e. mitophagy) with age. Thus, the purpose of our research was to evaluate mitochondrial content and function, along with rates of mitophagy, in the context of sarcopenic muscle loss. Consistent with previous studies (36, 44), we observed that aged animals displayed sarcopenia, accompanied by decrements in whole muscle mitochondrial volume. This occurred concomitant with the age-related reductions in endurance performance, accompanied by elevated lactic acid levels during exercise. In contrast to these changes in mitochondrial content, we detected no differences in glutamate-stimulated mitochondrial respiration rates between young and aged animals. Mitochondrial dysfunction is a common age-related outcome (3, 10, 31, 40), but it is not always observed in aged muscle (6, 22, 36, 47), likely a result, in part, of divergent physical activity patterns among aged cohorts (20).

Parkin is an E3 ubiquitin ligase selectively recruited to dysfunctional mitochondria during mitophagy (41). Under basal conditions, endogenous Parkin is predominately found in the cytosol (41, 57). During conditions of elevated mitochondrial stress, PINK1 stabilizes on the outer mitochondrial membrane and selectively recruits Parkin from the cytosol to activate it (42). Once activated, Parkin transfers ubiquitin onto outer mitochondrial membrane targets, such as Mfn2 (7, 12) and VDAC (13), to induce the removal of superfluous mitochondria. Mitophagy is a highly dynamic process that continually degrades superfluous, dysfunctional mitochondria within the cell. The measurement of autophagy pathway proteins at any given timepoint is acknowledged to provide only a snapshot that may not be representative of the process. As such, different inhibitors are commonly used to block certain steps of autophagy to measure flux. In our study, the microtubule-destabilizing drug colchicine was acutely injected intraperitoneally, thereby preventing autophagosomal transport to lysosomes for degradation (26). As a result, autophagy proteins did not degrade and accumulated in the cytosol, providing an indication of autophagic activity. It should be noted that a major challenge of measuring autophagy flux in vivo is the variability between animals. It is expected that different animals may not activate autophagy to the same degree. This increases the number of experiments that need to be performed to improve the statistical rigor of the findings.

It has been shown that autophagy is required to maintain muscle mass and myofiber integrity (38), and that overexpression of Parkin can positively impact longevity (21, 49). We observed no difference in muscle mass and mitochondrial content between young WT and Parkin KO animals, and there was no apparent additional decline in muscle or mitochondria in the absence of Parkin in aged animals. These findings indicate that the basal regulation of muscle mass is Parkin-independent. Interestingly, state 3 (active) mitochondrial respiration was significantly lower in young KO animals when compared to WT animals. Given that state 3 respiration is a surrogate measure for maximal ATP production in well-coupled mitochondria, KO mice should hypothetically have a lower maximal exercise capacity than WT mice. The lack of difference in running performance between young WT and KO mice, along with similar blood lactate levels, suggest the presence of a normal excess of mitochondrial capacity within muscle. However, we did observe an elevation in mitochondrial ROS production in aged KO animals. This is likely a consequence of altered glutamate-stimulated ETC complex I function in aged KO skeletal muscle, as others have reported that the absence of Parkin sensitizes complex I to oxidative stress (45) and mitochondrial toxins (50). This is consistent with a previous study showing that oxidative stress is exacerbated with a loss of Parkin activity in neuronal cells (59).

To further explore the physiological function of Parkin on mitophagy, we assessed Parkin's ability to translocate to mitochondria with exercise and age, as previous studies have shown that mitophagy may be required for exercise-induced remodeling of muscle (62). We did observe that mitochondrial localization of Parkin increased immediately following exercise in young WT animals, consistent with our previous study (62), but that this was attenuated with age. This observation, along with an increased expression of Parkin in aged muscle, suggests an impairment of Parkin translocation to the mitochondria with age and exercise. A similar attenuation in Parkin and its association with the organelle was documented in aged cardiac mouse muscle (21).

Upon mitochondrial depolarization, a multitude of outer mitochondrial membrane proteins are targeted for Parkin ubiquitination (54). Thus, our expectation was that basal ubiquitination would be reduced in the absence of Parkin. Although, we detected no differences in mitochondrial ubiquitin flux when multiple protein targets were evaluated, this result was not surprising as the existence of multiple ubiquitin ligases (e.g. MUL1 (66), MARCH5 (8), Gp78 (11)) can promote organelle ubiquitination, even in the absence of Parkin. Further scrutiny using a mitochondrial

co-immunoprecipitation assay of Mfn2, a bona fide target of Parkin (7, 12, 15), revealed a basal reduction of Mfn2-ubiquitin in young KO animals. This finding demonstrates that Parkin is required for basal organelle maintenance via ubiquitination. However, neither the absence of Parkin, nor the consequent reduction in target ubiquitination, were sufficient to impact mitophagic LC3II, p62 and ubiquitin flux in resting muscle. This suggests the existence of multiple mechanisms that compensate to determine basal mitophagic flux in Parkin KO animals.

During exercise, we found that Mfn2 ubiquitin flux was enhanced in young WT animals, and that this increase paralleled changes in LC3II and p62 flux, which corroborates previous studies showing that mitophagic flux is enhanced following an acute bout of exercise (62). Unexpectedly, this was also found during exercise in young KO animals, further supporting the existence of alternative unidentified E3 ubiquitin ligases that could be compensating for the lack of Parkin. However, these may not be sufficient, as exercise-induced mitophagic LC3II flux remained impaired in young KO animals.

With age, Parkin ubiquitination on general and specific OMM targets was enhanced, and remained unchanged in the absence of Parkin. Furthermore, age had an abating effect on exercise-induced ubiquitin signaling in aged animals. We speculate that this may be due to the altered activity of deubiquitinating enzymes (DUBs) contained on mitochondria and may be altered with age and/or exercise, which likely play a role in ubiquitin signaling and organelle degradation (1, 63). The attenuated exercise-induced ubiquitin signaling that we observed in our aging animals may be a fundamental characteristic of aging muscle, since we have previously observed reduced signaling in response to our experimental model of endurance exercise (35).

However, the requirement of Parkin and the effect of age on mitophagic flux in exercising muscle remains unknown. Under basal conditions, we did not detect a difference in mitophagic flux of LC3II, p62 and ubiquitin between young WT and KO animals. Our results did confirm an acute exercise-induced elevation of mitophagic LC3II flux in young animals, which was attenuated in the absence of Parkin. Interestingly, basal LC3II and p62 mitophagic flux were enhanced in aged WT muscle, and this was paralleled by greater generalized mitochondrial ubiquitination, as well as protein-specific (i.e. Mfn2) ubiquitination. This is in line with previous studies documenting reductions in Mfn2 protein abundance in aged muscle (23, 55). These data fortify the concept that Parkin and its association with OMM targets is altered with age. We extended these conclusions in an

aged exercising mouse model and found that the induction of LC3II and p62 mitophagic signaling with exercise was attenuated in aged muscle. This was likely due, in part, to an elevated baseline expression of these mitophagic proteins. Our data suggest that basal autophagosomal formation is not reduced with age, and that the increased expression and mitochondrial localization of ubiquitin, LC3II and p62 suggest the existence of accelerated mitophagy flux, at least up to the point of lysosomal degradation. Although definitive data do not yet exist in skeletal muscle, our previous results suggest the idea of defective lysosomal function with age. We have previously provided evidence that aged muscle displays lipofuscin granules within lysosomes, a clear indicator of lysosomal impairment (44). This supports the mitochondrial-lysosomal axis theory of aging (4), which hypothesizes that impairments in lysosomal activity may contribute to mitochondrial accumulation and dysfunction in aged post-mitotic tissue, such as muscle (6, 36, 44). The lysosome is a vital organelle for autophagosomal degradation, and its biogenesis is regulated by transcription factor EB (TFEB) (53). Roles for TFEB in mitochondrial turnover (43, 56) and exercise (29, 37) have been recently documented. However, future studies will need to examine the possibility of lysosomal biogenesis and function by examining possible differences in TFEB activation between young and aged animals.

In recent years, there has been mounting attention on identifying regulatory factors that can control the two opposing processes of mitochondrial biogenesis and mitophagy. Parkin is mainly implicated in mitophagy, but emerging work also indicates a role for Parkin in organelle biogenesis. For example, recent work has documented a potential Parkin-PARIS-PGC-1α relationship which could have implications for organelle synthesis. With a collapse in mitochondrial membrane potential, PARIS can localize on mitochondria where it is targeted for proteasomal degradation by PINK1 and Parkin (33). This can, in turn, diminish the repressive effect of PARIS on PGC-1α, permitting the transcription of nuclear genes encoding mitochondrial proteins (58) and improved cellular respiration (60). When Parkin is absent, it has been reported that PARIS can increase within the nucleus and transcriptionally repress PGC-1α (58, 60). Thus, an inverse relationship between Parkin and PARIS may exist, and have the potential to directly impact mitochondrial biogenesis. This presents a potential nexus for the regulation of mitochondrial biogenesis and degradation, and remains unexplored in the context of a physiologically relevant stressor such as exercise. Thus, we expected KO animals to display an elevation in PARIS and a decrease in PGC-1α. Interestingly, our results

illustrate a negative correlation between PARIS and PGC-1α localization in the nucleus that is dependent on exercise, and on the presence of Parkin in young animals. This reciprocal relationship was not visible under resting, basal conditions. However, with exercise the nuclear abundance of PGC-1α was increased in young WT animals, as reported by other studies (34, 51, 62, 64), and the nuclear translocation of PARIS was also enhanced with exercise, but only in young KO animals. This finding recapitulates previous work showing that nuclear PARIS levels increase with Parkin knockdown, and that it translocates into the nucleus under conditions of cellular stress (33). In aged muscle, we expected that elevated Parkin expression would repress PARIS and activate PGC-1α. In contrast, nuclear PARIS abundance was increased in aged muscle of both WT and KO animals, while the levels of nuclear PGC-1α were reduced. This likely contributes to the impaired transcriptional drive for mitochondrial biogenesis in aged muscle, leading to the decrements in mitochondrial content observed with age. Furthermore, recent research has also revealed that mitochondrial Parkin activation is required for PARIS degradation (33). Since Parkin localization to the organelle is attenuated with age, this may explain the enhanced nuclear localization of PARIS in aged muscle. These findings suggest an important Parkin-PARIS-PGC-1α axis that may be involved in muscle remodeling with exercise and warrants further investigation.

In summary, our data describe a role for Parkin-mediated mitochondrial degradation during exercise in muscle. Importantly, our study demonstrates that basal mitophagic flux is not depressed but rather enhanced with age, at least up to the level of the lysosome. We also show that acute exercise-induced mitophagic flux is dependent on Parkin, and that this exercise signaling is weakened with age. Additional studies are required to determine whether there is a direct connection between mitophagy flux and lysosomal activity with age, and whether chronic exercise can improve mitophagic flux along with changes in lysosomal capacity.

ACKNOWLEDGMENTS

The authors acknowledge Lucy Samoilov and Nemanja Dovijarski for their technical assistance during this study.

GRANTS

This work was supported by funding from the Natural Sciences and Engineering Research

Council (NSERC) of Canada grant (to D.A. Hood). D.A. Hood is the holder of a Canada Research Chair in Cell Physiology.

DISCLOSURES

No conflicts of interest, financial or otherwise, are declared by the author(s).

AUTHOR CONTRIBUTIONS

Author contributions: C.C.W.C., A.T.E. and M.J.C. performed experiments; C.C.W.C. analyzed data; C.C.W.C. and D.A.H. interpreted results of experiments; C.C.W.C. prepared figures; C.C.W.C. drafted manuscript; C.C.W.C. and D.A.H. edited and revised manuscript; C.C.W.C. and D.A.H. conception and design of research; C.C.W.C. and D.A.H. approved final version of manuscript.

REFERENCES

1. **Bingol B**, **Tea JS**, **Phu L**, **Reichelt M**, **Bakalarski CE**, **Song Q**, **Foreman O**, **Kirkpatrick DS**, **Sheng M**. The mitochondrial deubiquitinase USP30 opposes parkin-mediated mitophagy. *Nature* 510: 370–5, 2014.
2. **Bjørkøy G**, **Lamark T**, **Brech A**, **Outzen H**, **Perander M**, **Øvervatn A**, **Stenmark H**, **Johansen T**. p62/SQSTM1 forms protein aggregates degraded by autophagy and has a protective effect on huntingtin-induced cell death. *J Cell Biol* 171: 603–614, 2005.
3. **Boffoli D**, **Scacco SC**, **Vergari R**, **Solarino G**, **Santacroce G**, **Papa S**. Decline with age of the respiratory chain activity in human skeletal muscle. *Biochim Biophys Acta* 1226: 73–82, 1994.
4. **Brunk UT**, **Terman A**. The mitochondrial-lysosomal axis theory of aging: accumulation of damaged mitochondria as a result of imperfect autophagocytosis. *Eur J Biochem* 269: 1996–2002, 2002.
5. **Carter HN**, **Chen CCW**, **Hood DA**. Mitochondria, Muscle Health, and Exercise with Advancing Age. *Physiology* 30: 208–223, 2015.
6. **Chabi B**, **Ljubicic V**, **Menzies KJ**, **Huang JH**, **Saleem A**, **Hood DA**, **Aldridge JE**, **Horibe T**, **Hoogenraad NJ**. Mitochondrial function and apoptotic susceptibility in aging skeletal

muscle. *Aging Cell* 7: 2–12, 2008.

7. **Chen Y**, **Dorn GW**. PINK1-phosphorylated mitofusin 2 is a Parkin receptor for culling damaged mitochondria. *Science* 340: 471–5, 2013.

8. **Chen Z**, **Liu L**, **Cheng Q**, **Li Y**, **Wu H**, **Zhang W**, **Wang Y**, **Sehgal SA**, **Siraj S**, **Wang X**, **Wang J**, **Zhu Y**, **Chen Q**. Mitochondrial E3 ligase MARCH5 regulates FUNDC1 to fine-tune hypoxic mitophagy. *EMBO Rep* 18: 495–509, 2017.

9. **Cogswell AM**, **Stevens RJ**, **Hood DA**. Properties of skeletal muscle mitochondria isolated from subsarcolemmal and intermyofibrillar regions. *Am J Physiol* 264: C383-9, 1993.

10. **Cooper JM**, **Mann VM**, **Schapira AH**. Analyses of mitochondrial respiratory chain function and mitochondrial DNA deletion in human skeletal muscle: effect of ageing. *J Neurol Sci* 113: 91–8, 1992.

11. **Fu M**, **St-Pierre P**, **Shankar J**, **Wang PTC**, **Joshi B**, **Nabi IR**. Regulation of mitophagy by the Gp78 E3 ubiquitin ligase. *Mol Biol Cell* 24: 1153–62, 2013.

12. **Gegg ME**, **Cooper JM**, **Chau K-Y**, **Rojo M**, **Schapira AH V**, **Taanman J-W**. Mitofusin 1 and mitofusin 2 are ubiquitinated in a PINK1/parkin-dependent manner upon induction of mitophagy. *Hum Mol Genet* 19: 4861–70, 2010.

13. **Geisler S**, **Holmström KM**, **Skujat D**, **Fiesel FC**, **Rothfuss OC**, **Kahle PJ**, **Springer W**. PINK1/Parkin-mediated mitophagy is dependent on VDAC1 and p62/SQSTM1. *Nat Cell Biol* 12: 119–131, 2010.

14. **Goldberg MS**, **Fleming SM**, **Palacino JJ**, **Cepeda C**, **Lam HA**, **Bhatnagar A**, **Meloni EG**, **Wu N**, **Ackerson LC**, **Klapstein GJ**, **Gajendiran M**, **Roth BL**, **Chesselet M-FM-F**, **Maidment NT**, **Levine MS**, **Shen J**. Parkin-deficient mice exhibit nigrostriatal deficits but not loss of dopaminergic neurons. *J Biol Chem* 278: 43628–35, 2003.

15. **Gong G**, **Song M**, **Csordas G**, **Kelly DP**, **Matkovich SJ**, **Dorn GW**. Parkin-mediated mitophagy directs perinatal cardiac metabolic maturation in mice. *Science (80-)* 350: aad2459-aad2459, 2015.

16. **Greene JC**, **Whitworth AJ**, **Kuo I**, **Andrews LA**, **Feany MB**, **Pallanck LJ**. Mitochondrial pathology and apoptotic muscle degeneration in Drosophila parkin mutants. *Proc Natl Acad Sci U S A* 100: 4078–83, 2003.

17. **Grumati P**, **Coletto L**, **Schiavinato A**, **Castagnaro S**, **Bertaggia E**, **Sandri M**, **Bonaldo P**.

Physical exercise stimulates autophagy in normal skeletal muscles but is detrimental for collagen VI-deficient muscles. Taylor & Francis, 2011.

18. **He C**, **Bassik MC**, **Moresi V**, **Sun K**, **Wei Y**, **Zou Z**, **An Z**, **Loh J**, **Fisher J**, **Sun Q**, **Korsmeyer S**, **Packer M**, **May HI**, **Hill JA**, **Virgin HW**, **Gilpin C**, **Xiao G**, **Bassel-Duby R**, **Scherer PE**, **Levine B**. Exercise-induced BCL2-regulated autophagy is required for muscle glucose homeostasis. *Nature* 481: 511–5, 2012.
19. **Hood DA**. Invited Review: contractile activity-induced mitochondrial biogenesis in skeletal muscle. *J Appl Physiol* 90: 1137–57, 2001.
20. **Hood DA**, **Tryon LD**, **Carter HN**, **Kim Y**, **Chen CCW**. Unravelling the mechanisms regulating muscle mitochondrial biogenesis. *Biochem J* 473: 2295–2314, 2016.
21. **Hoshino A**, **Mita Y**, **Okawa Y**, **Ariyoshi M**, **Iwai-Kanai E**, **Ueyama T**, **Ikeda K**, **Ogata T**, **Matoba S**. Cytosolic p53 inhibits Parkin-mediated mitophagy and promotes mitochondrial dysfunction in the mouse heart. *Nat Commun* 4: 2308, 2013.
22. **Houtkooper RH**, **Argmann C**, **Houten SM**, **Cantó C**, **Jeninga EH**, **Andreux PA**, **Thomas C**, **Doenlen R**, **Schoonjans K**, **Auwerx J**. The metabolic footprint of aging in mice. *Sci Rep* 1: 134, 2011.
23. **Iqbal S**, **Ostojic O**, **Singh K**, **Joseph A-M**, **Hood DA**. Expression of mitochondrial fission and fusion regulatory proteins in skeletal muscle during chronic use and disuse. *Muscle Nerve* 48: 963–70, 2013.
24. **Janssen I**, **Heymsfield SB**, **Ross R**. Low relative skeletal muscle mass (sarcopenia) in older persons is associated with functional impairment and physical disability. *J Am Geriatr Soc* 50: 889–96, 2002.
25. **Jin SM**, **Lazarou M**, **Wang C**, **Kane LA**, **Narendra DP**, **Youle RJ**. Mitochondrial membrane potential regulates PINK1 import and proteolytic destabilization by PARL. *J Cell Biol* 191: 933–42, 2010.
26. **Ju J-S**, **Varadhachary AS**, **Miller SE**, **Weihl CC**. Quantitation of "autophagic flux" in mature skeletal muscle. *Autophagy* 6: 929–935, 2010.
27. **Kane LA**, **Lazarou M**, **Fogel AI**, **Li Y**, **Yamano K**, **Sarraf SA**, **Banerjee S**, **Youle RJ**. PINK1 phosphorylates ubiquitin to activate Parkin E3 ubiquitin ligase activity. *J Cell Biol* 205: 143–53, 2014.

28. **Kazlauskaite A**, **Kondapalli C**, **Gourlay R**, **Campbell DG**, **Ritorto MS**, **Hofmann K**, **Alessi DR**, **Knebel A**, **Trost M**, **Muqit MMK**. Parkin is activated by PINK1-dependent phosphorylation of ubiquitin at Ser 65. *Biochem J* 460: 127–139, 2014.

29. **Kim Y**, **Hood DA**. Regulation of the autophagy system during chronic contractile activity-induced muscle adaptations. *Physiol Rep* 5: e13307, 2017.

30. **Koyano F**, **Okatsu K**, **Kosako H**, **Tamura Y**, **Go E**, **Kimura M**, **Kimura Y**, **Tsuchiya H**, **Yoshihara H**, **Hirokawa T**, **Endo T**, **Fon EA**, **Trempe J-F**, **Saeki Y**, **Tanaka K**, **Matsuda N**. Ubiquitin is phosphorylated by PINK1 to activate parkin. *Nature* 510: 162–6, 2014.

31. **Kruse SE**, **Karunadharma PP**, **Basisty N**, **Johnson R**, **Beyer RP**, **MacCoss MJ**, **Rabinovitch PS**, **Marcinek DJ**. Age modifies respiratory complex I and protein homeostasis in a muscle type-specific manner. *Aging Cell* 15: 89–99, 2016.

32. **Lazarou M**, **Jin SM**, **Kane LA**, **Youle RJ**. Role of PINK1 binding to the TOM complex and alternate intracellular membranes in recruitment and activation of the E3 ligase Parkin. *Dev Cell* 22: 320–33, 2012.

33. **Lee Y**, **Stevens DA**, **Kang S-U**, **Jiang H**, **Lee Y-I**, **Ko HS**, **Scarffe LA**, **Umanah GE**, **Kang H**, **Ham S**, **Kam T-I**, **Allen K**, **Brahmachari S**, **Kim JW**, **Neifert S**, **Yun SP**, **Fiesel FC**, **Springer W**, **Dawson VL**, **Shin J-H**, **Dawson TM**. PINK1 Primes Parkin-Mediated Ubiquitination of PARIS in Dopaminergic Neuronal Survival. *Cell Rep* 18: 918–932, 2017.

34. **Little JP**, **Safdar A**, **Cermak N**, **Tarnopolsky MA**, **Gibala MJ**. Acute endurance exercise increases the nuclear abundance of PGC-1 in trained human skeletal muscle. *AJP Regul Integr Comp Physiol* 298: R912–R917, 2010.

35. **Ljubicic V**, **Hood DA**. Diminished contraction-induced intracellular signaling towards mitochondrial biogenesis in aged skeletal muscle. *Aging Cell* 8: 394–404, 2009.

36. **Ljubicic V**, **Joseph A-M**, **Adhihetty PJ**, **Huang JH**, **Saleem A**, **Uguccioni G**, **Hood DA**. Molecular basis for an attenuated mitochondrial adaptive plasticity in aged skeletal muscle. *Aging (Albany NY)* 1: 818–30, 2009.

37. **Mansueto G**, **Armani A**, **Viscomi C**, **D'Orsi L**, **De Cegli R**, **Polishchuk E V**, **Lamperti C**, **Di Meo I**, **Romanello V**, **Marchet S**, **Saha PK**, **Zong H**, **Blaauw B**, **Solagna F**, **Tezze C**, **Grumati P**, **Bonaldo P**, **Pessin JE**, **Zeviani M**, **Sandri M**, **Ballabio A**. Transcription Factor EB Controls Metabolic Flexibility during Exercise. *Cell Metab* 25: 182–196, 2017.

38. **Masiero E**, **Agatea L**, **Mammucari C**, **Blaauw B**, **Loro E**, **Komatsu M**, **Metzger D**, **Reggiani C**, **Schiaffino S**, **Sandri M**. Autophagy is required to maintain muscle mass. *Cell Metab* 10: 507–15, 2009.

39. **Menzies KJ**, **Singh K**, **Saleem A**, **Hood DA**. Sirtuin 1-mediated effects of exercise and resveratrol on mitochondrial biogenesis. *J Biol Chem* 288: 6968–79, 2013.

40. **Nabben M**, **Hoeks J**, **Briedé JJ**, **Glatz JFC**, **Moonen-Kornips E**, **Hesselink MKC**, **Schrauwen P**. The effect of UCP3 overexpression on mitochondrial ROS production in skeletal muscle of young versus aged mice. *FEBS Lett* 582: 4147–4152, 2008.

41. **Narendra D**, **Tanaka A**, **Suen D-F**, **Youle RJ**. Parkin is recruited selectively to impaired mitochondria and promotes their autophagy. *J Cell Biol* 183: 795–803, 2008.

42. **Narendra DP**, **Jin SM**, **Tanaka A**, **Suen D-F**, **Gautier CA**, **Shen J**, **Cookson MR**, **Youle RJ**. PINK1 is selectively stabilized on impaired mitochondria to activate Parkin. *PLoS Biol* 8: e1000298, 2010.

43. **Nezich CL**, **Wang C**, **Fogel AI**, **Youle RJ**. MiT/TFE transcription factors are activated during mitophagy downstream of Parkin and Atg5. *J Cell Biol* 210: 435–450, 2015.

44. **O'Leary MF**, **Vainshtein A**, **Iqbal S**, **Ostojic O**, **Hood DA**. Adaptive plasticity of autophagic proteins to denervation in aging skeletal muscle. *Am J Physiol Cell Physiol* 304: C422-30, 2013.

45. **Palacino JJ**, **Sagi D**, **Goldberg MS**, **Krauss S**, **Motz C**, **Wacker M**, **Klose J**, **Shen J**. Mitochondrial Dysfunction and Oxidative Damage in *parkin* -deficient Mice. *J Biol Chem* 279: 18614–18622, 2004.

46. **Pankiv S**, **Clausen TH**, **Lamark T**, **Brech A**, **Bruun J-A**, **Outzen H**, **Øvervatn A**, **Bjørkøy G**, **Johansen T**. p62/SQSTM1 Binds Directly to Atg8/LC3 to Facilitate Degradation of Ubiquitinated Protein Aggregates by Autophagy. *J Biol Chem* 282: 24131–24145, 2007.

47. **Picard M**, **Ritchie D**, **Thomas MM**, **Wright KJ**, **Hepple RT**. Alterations in intrinsic mitochondrial function with aging are fiber type-specific and do not explain differential atrophy between muscles. *Aging Cell* 10, 2011.

48. **Poole AC**, **Thomas RE**, **Andrews LA**, **McBride HM**, **Whitworth AJ**, **Pallanck LJ**. The PINK1/Parkin pathway regulates mitochondrial morphology. *Proc Natl Acad Sci* 105: 1638–1643, 2008.

49. **Rana A**, **Rera M**, **Walker DW**. Parkin overexpression during aging reduces proteotoxicity, alters mitochondrial dynamics, and extends lifespan. *Proc Natl Acad Sci U S A* 110: 8638–43, 2013.

50. **Rosen KM**, **Veereshwarayya V**, **Moussa CE-H**, **Fu Q**, **Goldberg MS**, **Schlossmacher MG**, **Shen J**, **Querfurth HW**. Parkin Protects against Mitochondrial Toxins and β-Amyloid Accumulation in Skeletal Muscle Cells. *J Biol Chem* 281: 12809–12816, 2006.

51. **Saleem A**, **Carter HN**, **Hood DA**. p53 is necessary for the adaptive changes in cellular milieu subsequent to an acute bout of endurance exercise. 306: C241-9, 2014.

52. **Saleem A**, **Iqbal S**, **Zhang Y**, **Hood DA**. Effect of p53 on mitochondrial morphology, import, and assembly in skeletal muscle. *Am J Physiol - Cell Physiol* 308, 2015.

53. **Sardiello M**, **Palmieri M**, **di Ronza A**, **Medina DL**, **Valenza M**, **Gennarino VA**, **Di Malta C**, **Donaudy F**, **Embrione V**, **Polishchuk RS**, **Banfi S**, **Parenti G**, **Cattaneo E**, **Ballabio A**. A Gene Network Regulating Lysosomal Biogenesis and Function. *Science (80-)* 325: 473–7, 2009.

54. **Sarraf SA**, **Raman M**, **Guarani-Pereira V**, **Sowa ME**, **Huttlin EL**, **Gygi SP**, **Harper JW**. Landscape of the PARKIN-dependent ubiquitylome in response to mitochondrial depolarization. *Nature* 496: 372–6, 2013.

55. **Sebastián D**, **Sorianello E**, **Segalés J**, **Irazoki A**, **Ruiz-Bonilla V**, **Sala D**, **Planet E**, **Berenguer-Llergo A**, **Muñoz JP**, **Sánchez-Feutrie M**, **Plana N**, **Hernández-Álvarez MI**, **Serrano AL**, **Palacín M**, **Zorzano A**. Mfn2 deficiency links age-related sarcopenia and impaired autophagy to activation of an adaptive mitophagy pathway. *EMBO J* 35: 1677–93, 2016.

56. **Settembre C**, **Di Malta C**, **Polito VA**, **Garcia Arencibia M**, **Vetrini F**, **Erdin SUSU**, **Erdin SUSU**, **Huynh T**, **Medina D**, **Colella P**, **Sardiello M**, **Rubinsztein DC**, **Ballabio A**, **Arencibia MG**, **Vetrini F**, **Erdin SUSU**, **Erdin SUSU**, **Huynh T**, **Medina D**, **Colella P**, **Sardiello M**, **Rubinsztein DC**, **Ballabio A**. TFEB links autophagy to lysosomal biogenesis. *Science* 332: 1429–33, 2011.

57. **Shimura H**, **Hattori N**, **Kubo S**, **Yoshikawa M**, **Kitada T**, **Matsumine H**, **Asakawa S**, **Minoshima S**, **Yamamura Y**, **Shimizu N**, **Mizuno Y**. Immunohistochemical and subcellular localization of Parkin protein: absence of protein in autosomal recessive juvenile

parkinsonism patients. *Ann Neurol* 45: 668–72, 1999.

58. **Shin J-H**, **Ko HS**, **Kang H**, **Lee Y**, **Lee Y-I**, **Pletinkova O**, **Troconso JC**, **Dawson VL**, **Dawson TM**. PARIS (ZNF746) repression of PGC-1α contributes to neurodegeneration in Parkinson's disease. *Cell* 144: 689–702, 2011.

59. **Siddiqui A**, **Rane A**, **Rajagopalan S**, **Chinta SJ**, **Andersen JK**. Detrimental effects of oxidative losses in parkin activity in a model of sporadic Parkinson's disease are attenuated by restoration of PGC1alpha. *Neurobiol Dis* 93: 115–120, 2016.

60. **Stevens DA**, **Lee Y**, **Kang HC**, **Lee BD**, **Lee Y-I**, **Bower A**, **Jiang H**, **Kang S-U**, **Andrabi SA**, **Dawson VL**, **Shin J-H**, **Dawson TM**. Parkin loss leads to PARIS-dependent declines in mitochondrial mass and respiration. *Proc Natl Acad Sci U S A* 112: 11696–701, 2015.

61. **Twig G**, **Elorza A**, **Molina AJA**, **Mohamed H**, **Wikstrom JD**, **Walzer G**, **Stiles L**, **Haigh SE**, **Katz S**, **Las G**, **Alroy J**, **Wu M**, **Py BF**, **Yuan J**, **Deeney JT**, **Corkey BE**, **Shirihai OS**. Fission and selective fusion govern mitochondrial segregation and elimination by autophagy. *EMBO J* 27: 433–446, 2008.

62. **Vainshtein A**, **Tryon LD**, **Pauly M**, **Hood DA**. Role of PGC-1α during acute exercise-induced autophagy and mitophagy in skeletal muscle. *Am J Physiol Cell Physiol* 308: C710-9, 2015.

63. **Wang Y**, **Serricchio M**, **Jauregui M**, **Shanbhag R**, **Stoltz T**, **Di Paolo CT**, **Kim PK**, **McQuibban GA**. Deubiquitinating enzymes regulate PARK2-mediated mitophagy. *Autophagy* 11: 595–606, 2015.

64. **Wright DC**, **Han D-H**, **Garcia-Roves PM**, **Geiger PC**, **Jones TE**, **Holloszy JO**. Exercise-induced mitochondrial biogenesis begins before the increase in muscle PGC-1alpha expression. *J Biol Chem* 282: 194–9, 2007.

65. **Youle RJ**, **van der Bliek AM**. Mitochondrial Fission, Fusion, and Stress. *Science (80-)* 337: 1062–1065, 2012.

66. **Yun J**, **Puri R**, **Yang H**, **Lizzio MA**, **Wu C**, **Sheng Z-H**, **Guo M**. MUL1 acts in parallel to the PINK1/parkin pathway in regulating mitofusin and compensates for loss of PINK1/parkin. *Elife* 3: e01958, 2014.

67. **Zhang Y**, **Iqbal S**, **O'Leary MFN**, **Menzies KJ**, **Saleem A**, **Ding S**, **Hood DA**. Altered mitochondrial morphology and defective protein import reveal novel roles for Bax and/or Bak

715 in skeletal muscle. *Am J Physiol Cell Physiol* 305: C502-11, 2013.

716

717

718

719

FIGURE LEGENDS

Fig. 1. Effect of aging and Parkin deficiency on mitochondrial content and function. (*A)*: Representative Western blot of Parkin expression in young (*Y*) and aged (*A*) skeletal muscle of control wild-type (WT) mice above. A graphical representation is shown below (n = 4). (*B)*: Cytochrome c oxidase (COX) activity in quadriceps muscle of young and aged Parkin KO and WT animals (n = 6). *(C)*: Mitochondrial state 4 and state 3 respiration rates in KO compared with WT animals (n = 6–9, ¶P < 0.05, vs young WT state 3). (*D*): Mitochondrial ROS production expressed per natom of oxygen consumed in Parkin KO and WT mice (n = 6–9, #P < 0.05, vs remaining state 4 conditions). Values are means ± SEM. *P < 0.05, main effect of age. WT, wild-type; KO, Parkin knock-out; A.U., arbitrary units.

Fig. 2. Effect of Parkin and age on exercise performance. (*A*): Representative Western blot of Parkin localization on isolated mitochondria from young and aged WT muscle, prior to exercise (Con) and immediately following exercise (Ex). Quantification of mitochondrial Parkin localization is shown below, corrected for loading using mitochondrial voltage-dependent anion channel (VDAC) (n = 3). (*B*): Animal performance (i.e. total distance run) of WT and KO mice injected with water (Veh) or 0.4 mg/kg colchicine (Col) (n = 6–8). (*C*): Blood lactate levels measured prior to (Con), and immediately following exercise (Ex) (n = 6–8). Values are means ± SEM. †P < 0.05, interaction effect of exercise and age. *P < 0.05, main effect of age. ¶P < 0.05, vs young Con. #P < 0.05, significant difference from aged WT mice. WT, wild-type; KO, Parkin knock-out; A.U., arbitrary units.

Fig. 3. Mitophagy flux following an acute bout of exercise in young Parkin KO and WT mice. (*A*): Representative Western blots of LC3II and p62 localization on isolated mitochondria from WT and KO mice injected with water (Veh) or 0.4 mg/kg colchicine (Col). Quantification of LC3II (*B*) and p62 (*C*) mitochondrial localization is shown (n = 7). Mitophagy flux of LC3II (*D*) and p62 (*E*) were assessed prior to exercise (C), immediately following exercise (Ex), and following 2 hours of recovery (ExR). Values are means ± SEM. ¶P< 0.05, vs WT Con. Voltage-dependent anion channel (VDAC) was used as a mitochondrial loading control. WT, wild-type; KO, Parkin knock-out; LC3II, lipidated microtubule-associated protein 1A/1B-light chain 3; p62, sequestosome 1; A.U., arbitrary units.

Fig. 4. Mitophagy flux following an acute bout of exercise in young and aged Parkin KO and WT mice. (*A*): Representative Western blots of LC3II and p62 localization on isolated mitochondria from young and aged WT injected with water (Veh) or 0.4 mg/kg colchicine (Col). Quantification of mitochondrial LC3II flux (*B*) and p62 flux (*C*) is shown ($n = 6$). (*D*): Representative Western blots of LC3II and p62 localization on isolated mitochondria from young and aged KO injected with water [Veh (Vehicle)] or 0.4 mg/kg colchicine (Col). Mitochondrial LC3II flux (*E*) and p62 flux (*F*) with age and exercise are quantified ($n = 6$). Quantification of basal LC3II flux (*G*) and p62 flux (*H*) with age only. Mitophagy flux and localization of LC3II and p62 were assessed prior to exercise (C) and immediately following exercise (Ex). Values are means ± SEM. *$P < 0.05$, main effect of age. ¶$P < 0.05$, main effect of exercise. #$P < 0.05$, significant difference from aged WT mice. Voltage-dependent anion channel (VDAC) was used as a mitochondrial loading control. WT, wild-type; KO, Parkin knock-out; LC3II, lipidated microtubule-associated protein 1A/1B-light chain 3; p62, sequestosome 1; A.U., arbitrary units.

Fig. 5. Mitochondrial ubiquitination following an acute bout of exercise in young and aged Parkin KO and WT mice. (*A*): Representative Western blot of ubiquitin (Ub) on isolated mitochondria from young WT and KO mice injected with water (Veh) or 0.4 mg/kg colchicine (Col). (*B*): Quantification of mitochondrial Ub flux in young WT and KO mice ($n = 8$). (*C*): Representative Western blot of ubiquitin (Ub) on isolated mitochondria from aged WT and KO mice injected with water (Veh) or 0.4 mg/kg colchicine (Col). (*D*): Quantification of mitochondrial Ub flux in aged WT and KO mice ($n = 6$). (*E*): Mfn2 was immunoprecipitated (IP) followed by immunoblotting (IB) for ubiquitin on isolated mitochondria from young and aged groups of Parkin KO and WT animals prior to, and immediately following exercise. (*F*): Graphical representation of mitochondrial Mfn2 ubiquitination relative to young WT control values ($n = 6$). In young animals, mitochondrial Ub flux was assessed prior to exercise (C), immediately following exercise (Ex), and following 2 hours of recovery (ExR). There was no recovery group for the aged animals in the measurement of mitochondrial ubiquitination following exercise (*C*–*F*). Values are means ± SEM. ¶$P < 0.05$, main effect of exercise. #$P < 0.05$, vs young WT Con. Voltage-dependent anion channel (VDAC) was used as a mitochondrial loading control. Immunoglobulin G (IgG) was used as a negative control for co-immunoprecipitation

validation. WT, wild-type; KO, Parkin knock-out; Ub, ubiquitin; Mfn2, Mitofusin-2; IgG, Immunoglobulin G; A.U., arbitrary units.

Fig. 6. Effect of Parkin and age on PARIS and PGC-1α nuclear translocation. (*A*): Representative Western blots for PARIS, PGC-1α, H2B and α-tubulin. (*B*): Graphical quantification of [nuclear (N)] PARIS represented as a percentage of total [cytosol (C) + nuclear (N)] PARIS (n = 6). (*C*): PGC-1α nuclear abundance (n = 6). Values are means ± SEM. *P < 0.05, main effect of age. #P < 0.05, significant difference from aged mice. Nuclear and cytosol protein expression were corrected for loading using nuclear histone 2B (H2B) and α-tubulin, respectively. PARIS, Parkin-Interacting Substrate; PGC-1α, peroxisome proliferator gamma coactivator-1α.

Fig. 7. Effect of Parkin and age on exercise-induced PARIS and PGC-1α subcellular localization. (*A*) and (*B*): Representative Western blots for PARIS, PGC-1α, H2B and α-tubulin are shown. Graphical representation of [nuclear (N)] PARIS represented as a percentage of total [cytosol (C) + nuclear (N)] PARIS in young (*C*) and aged (*D*) mice (n = 5–8). Graphical quantification of PGC-1α in nuclear fraction of young (*E*) and aged (*F*) animals (n = 6–7). In young animals, measurements of PARIS (*C*) and PGC-1α (*E*) were done prior to exercise (Con), immediately following exercise (Ex), and following 2 hours of recovery (ExR). There was no recovery group for aged animals in the evaluation of PARIS (*D*) and PGC-1α (*F*) subcellular localization following exercise. Values are means ± SEM. †P < 0.05, interaction effect of exercise and genotype. ¶P < 0.05, vs WT Con. Histone 2B (H2B) was used as a nuclear loading control and α-tubulin was used as a cytosol loading control. PARIS, Parkin-Interacting Substrate; PGC-1α, peroxisome proliferator gamma coactivator-1α; WT, wild-type; KO, Parkin knock-out.

Table 1. Animal characteristics of WT and Parkin KO mice

Condition	Young WT	Aged WT	Young KO	Aged KO
Body Mass, g	31.4 ± 3.4	49.7 ± 3.3*	27.2 ± 2.6	49.8 ± 1.0*
Quadriceps Mass, mg	237.8 ± 27.0	191.9 ± 11.5	187.1 ± 22.4	156.3 ± 11.7
Quadriceps Mass / Body Mass, mg/g	7.3 ± 0.3	4.0 ± 0.4*	6.7 ± 0.3	3.1 ± 0.2*
Heart Mass, mg	166.0 ± 6.4	192.9 ± 8.1	143.3 ± 16.3	184.8 ± 13.1
Heart Mass / Body Mass, mg/g	5.5 ± 0.5	4.0 ± 0.3*	5.4 ± 0.6	3.7 ± 0.3*
Epididymal Fat Mass, g	0.17 ± 0.01	2.41 ± 0.19*	0.15 ± 0.01	2.09 ± 0.17*
Epididymal Fat Mass / Body Mass, mg/g	5.9 ± 0.9	50.6 ± 6.5*	5.6 ± 0.4	42.0 ± 3.1*
Tibia length (mm)	21.7 ± 0.3	21.6 ± 0.9	21.2 ± 0.7	21.1 ± 0.6
Quadriceps Mass / Tibia Length, mg/mm	11.0 ± 1.2	8.9 ± 0.5*	8.8 ± 1.1	7.4 ± 0.6
Quadriceps Mass / Tibia Length (aged over young)	0.87 ± 0.12		0.89 ± 0.11	

Values are reported as means ± SEM, $n = 6$. * $P < 0.05$ vs. Young counterpart

Figure 1

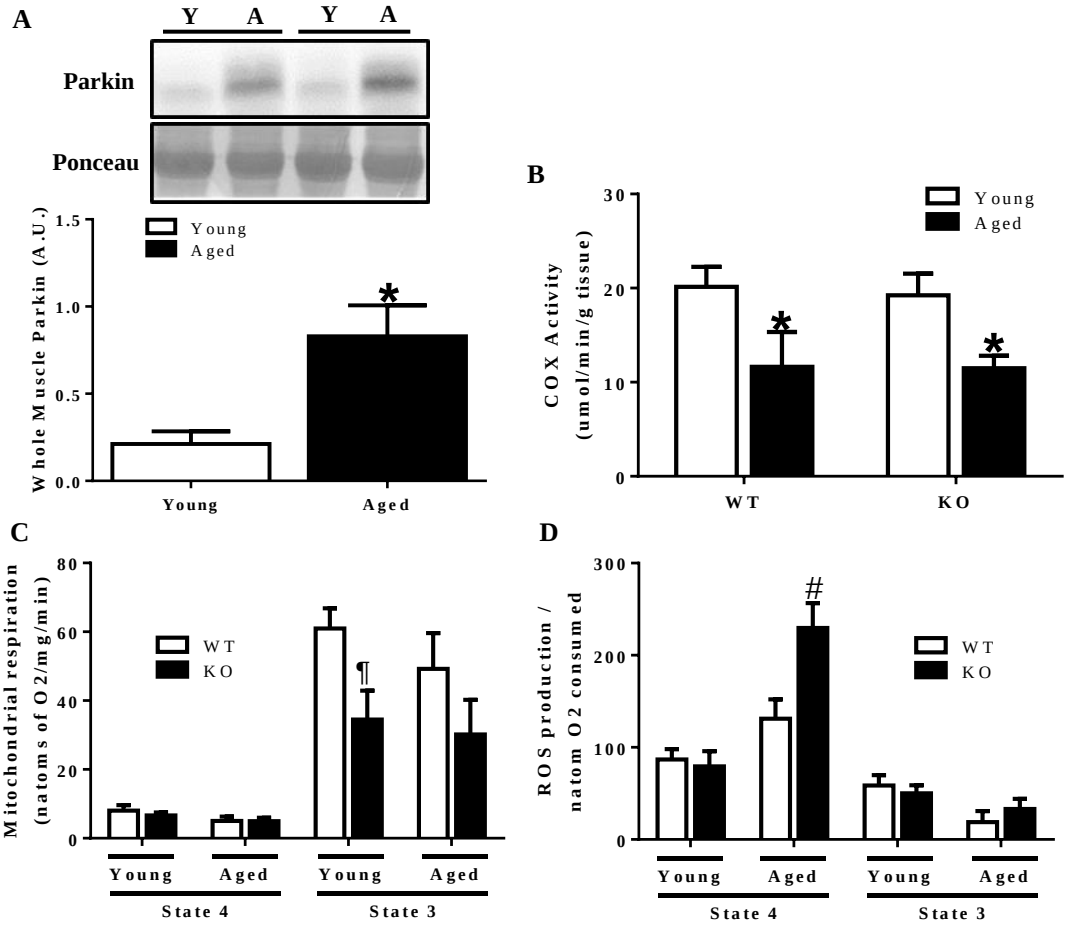

Figure 2

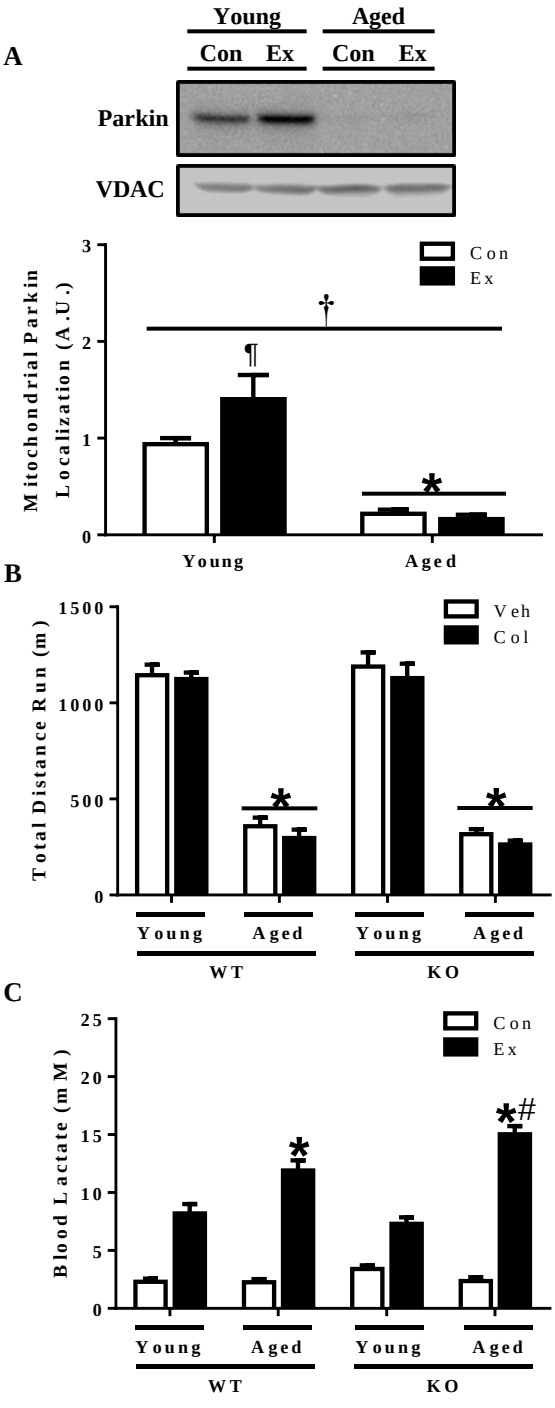

Figure 3

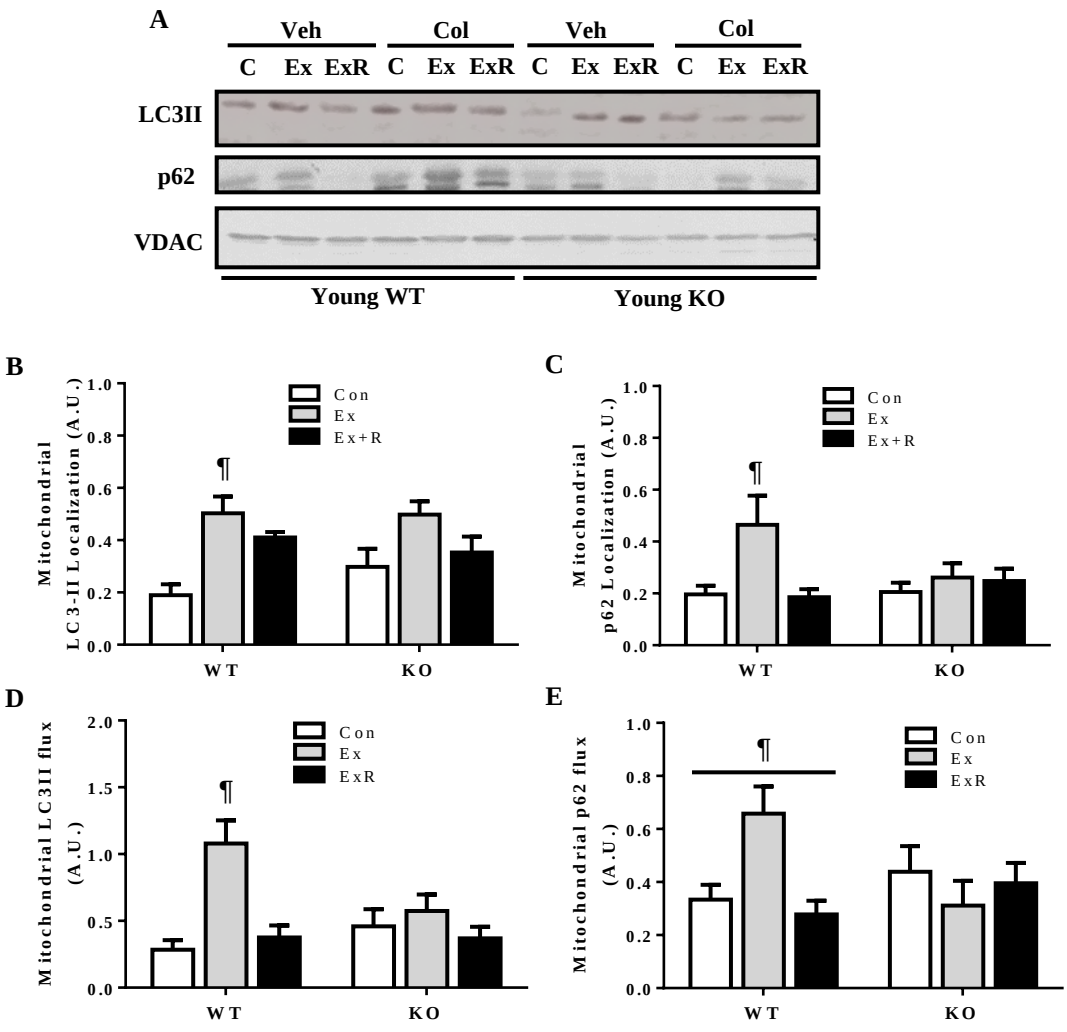

Figure 4

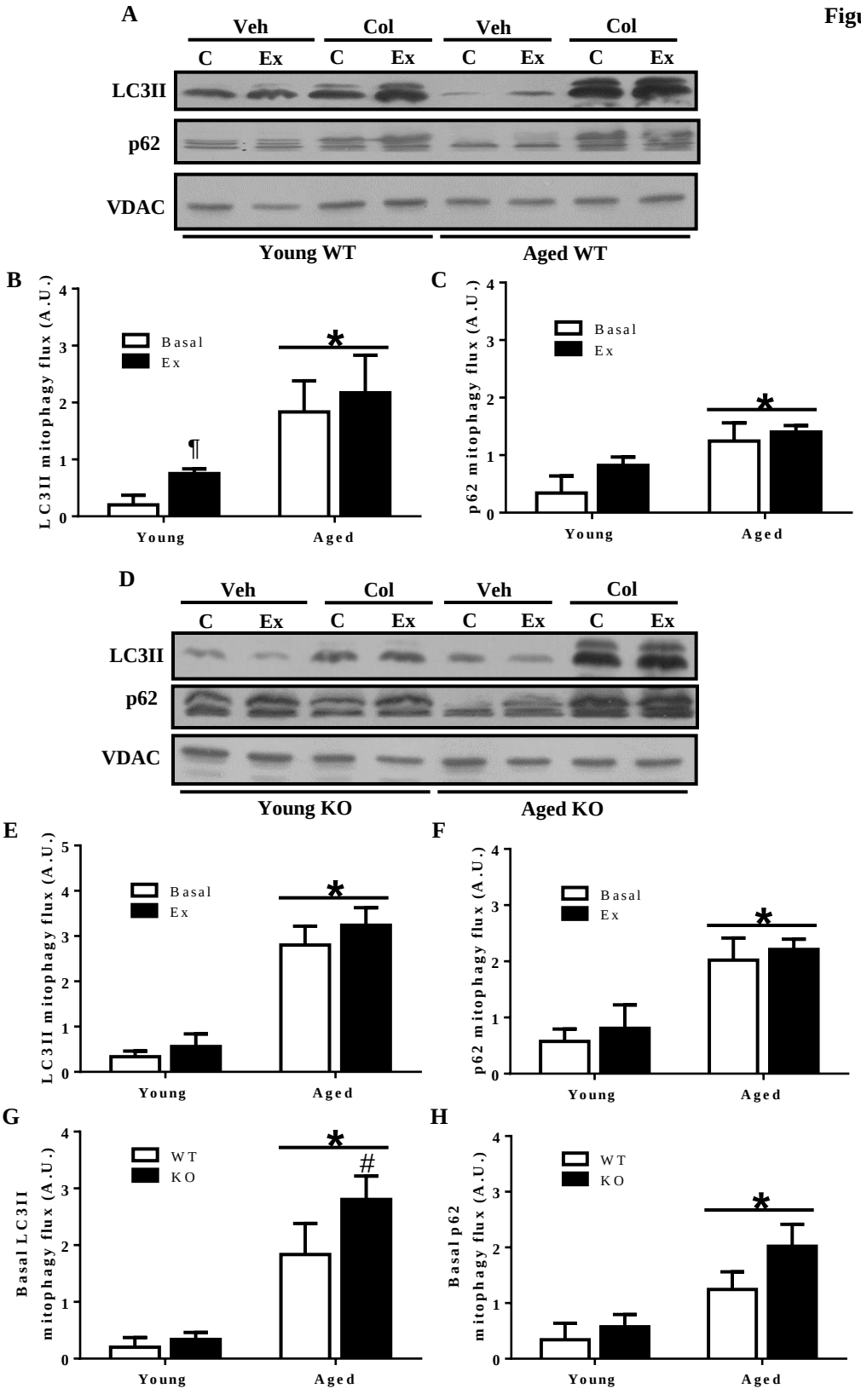

Figure 5

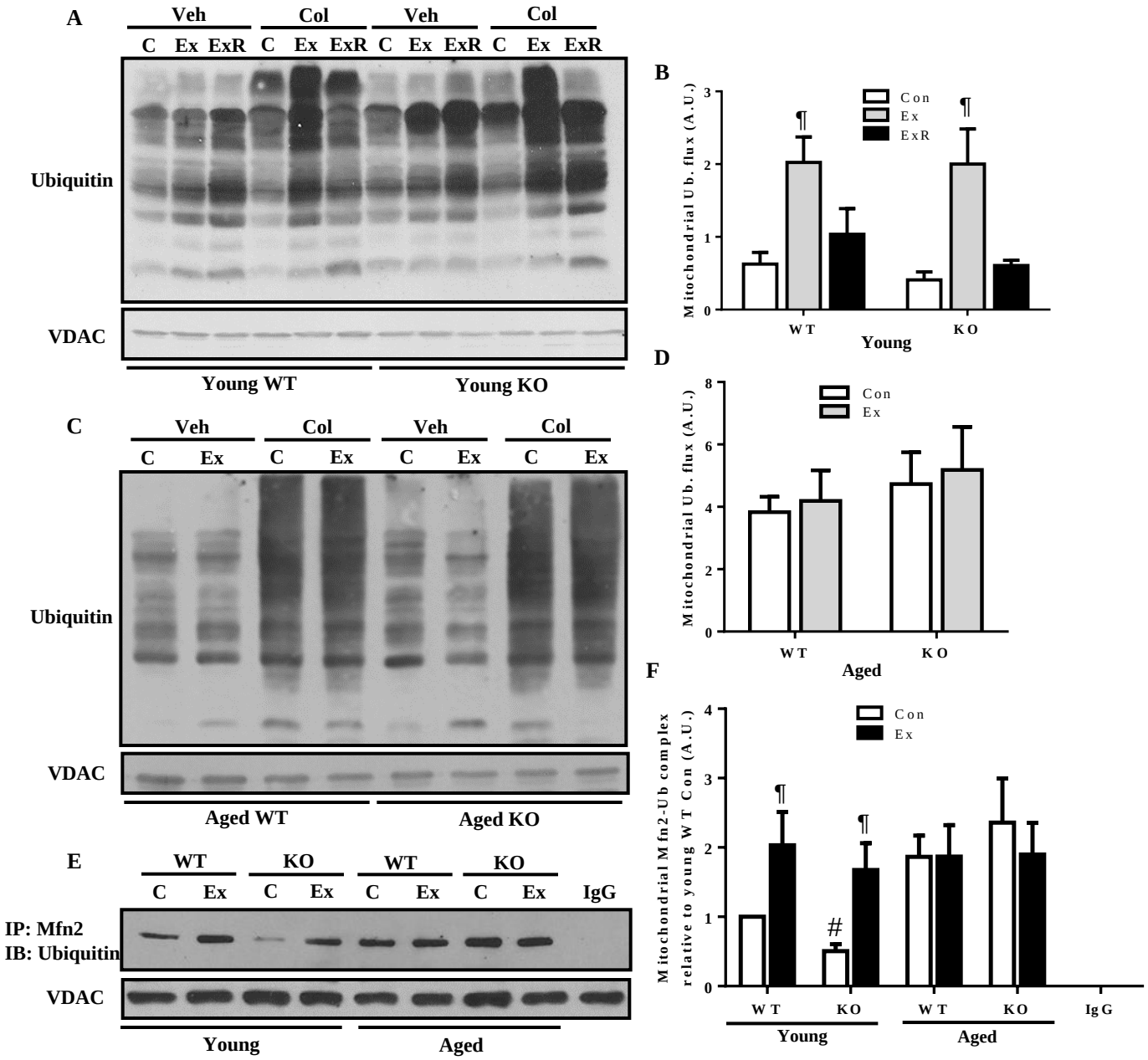

Figure 6

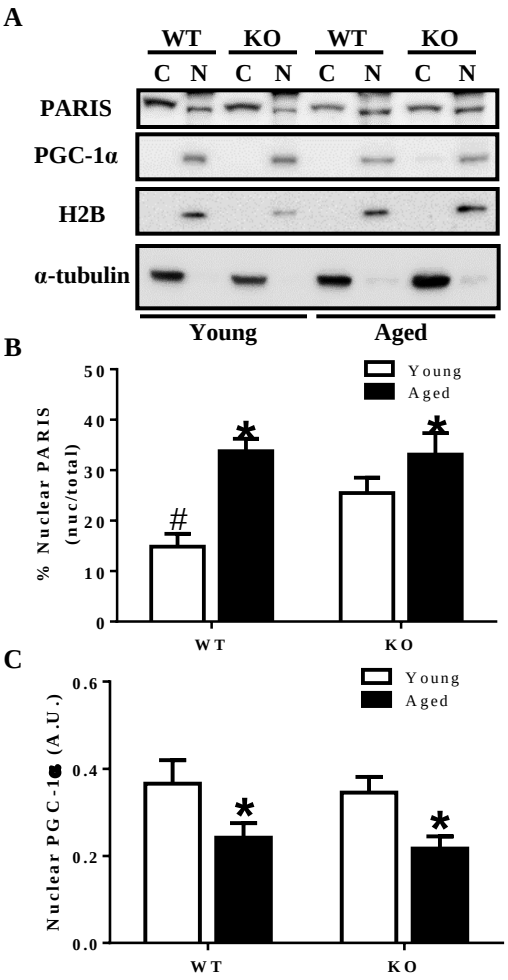

Figure 7